Electronic phase diagram of Li_xCoO_2 revisited with potentiostatically de-intercalated single crystals

T. Y. Ou-Yang[1,2], F. -T. Huang[1], G. J. Shu[1], W. L. Lee[3], M. -W. Chu[1], H. L. Liu[2], and F. C. Chou[1,4*]
[1] *Center for Condensed Matter Sciences, National Taiwan University, Taipei 10617, Taiwan*
[2] *Department of Physics, National Taiwan Normal University, Taipei 11677, Taiwan*
[3] *Institute of Physics, Academia Sinica, Taipei 11529, Taiwan and*
[4] *National Synchrotron Radiation Research Center, Hsinchu 30076, Taiwan*
(Dated: January 12, 2012)

Electronic phase diagram of Li_xCoO_2 has been re-examined using potentiostatically de-intercalated single crystal samples. Stable phases of x ∼ 0.87, 0.72, 0.53, 0.50, 0.43, and 0.33 were found and isolated for physical property studies. A-type and chain-type antiferromagnetic orderings have been suggested from magnetic susceptibility measurement results in x ∼ 0.87 and 0.50 below ∼ 10K and 200K, respectively, similar to those found in Na_xCoO_2 system. There is no Li vacancy superlattice ordering observed at room temperature for the electronically stable phase $Li_{0.72}CoO_2$ as revealed by synchrotron X-ray Laue diffraction. The peculiar magnetic anomaly near ∼175K as often found in powder samples of x∼0.46-0.78 cannot be isolated through this single crystal potentiostatic method, which supports the previously proposed explanation to be surface stabilized phase of significant thermal hysteresis and aging character.

PACS numbers: 75.25.-j, 75.30.Gw, 61.72.jd, 63.22.Np, 71.30.+h, 74.62.Bf

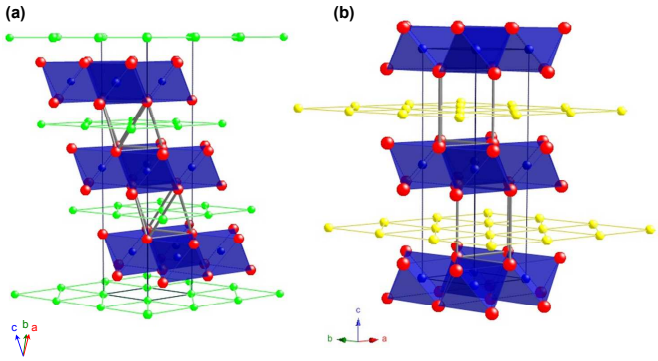

FIG. 1. (color online) Crystal structures of (a) O3-Li_xCoO_2 described by rhombohedral R$\bar{3}$m or trigonal layer symmetry and (b) P2-Na_xCoO_2 described by $P6_3/mmc$ symmetry are compared. Note that Li_xCoO_2 has three glide layers of LiO_6 octahedral per unit as drawn in hexagonal form, and there are two reversed layers of NaO_6 trigonal prismatic per unit.

I. INTRODUCTION

Both layered P2-Na_xCoO_2 (also called γ-phase) and O3-Li_xCoO_2 (also called α-phase) compounds have been investigated intensely as a rechargeable battery electrode material, and the latter, in particular, has been commercialized, based on its proper application voltage, high energy density, and high rate capacity.[1] In general, both systems are composed of alternating layers of CoO_2 and alkali metal with 2D hexagonal symmetry. As illustrated in Fig. 1, the major difference lies in the oxygen coordination near the cations, i.e., P2-Na_xCoO_2 can be described by $P6_3/mmc$ space group with two opposite prismatic NaO_6 layers (P2) sandwiched between Co-layers per unit, while Li_xCoO_2 shows rhombohedral R$\bar{3}$m or trigonal layer symmetry with three gliding layers of LiO_6 octahedra (O3) sandwiched in between Co-layers per unit when drawn in hexagonal form.[2] The surprising finding of superconductivity in $Na_xCoO_2{\cdot}yH_2O$ (x ∼ 1/3 and y ∼ 4/3) has generated intense investigation on the rich electronic phase digram of Na_xCoO_2, including antiferromagnetic ordering, metal-insulator transition, and superconductivity.[3,4] On the other hand, detailed Li_xCoO_2 electronic phase diagram remains to be illusive while being hindered by the availability of sizable high quality single crystal samples with well-controlled homogeneous Li content.

Na vacancy cluster ordering in layered Na_xCoO_2 has been shown to be a fascinating phenomenon since the various superstructures were observed through neutron and synchrotron X-ray diffraction techniques.[5,6] The strong correlation between vacancy cluster ordering pattern and the distinct physical properties at specific x values has been explored in detailed since.[7,8] However, although similar characteristic surface potential V vs. x behaviors have been found in the nearly isostructural Li_xCoO_2 through repeated electrochemical galvanostatic charge/discharge scans, both in-situ and ex-situ, the expected similar Li vacancy orderings from the nearly isostructural Li_xCoO_2 have been implied yet never observed with solid evidence.[2,9] While the existence of electronically stable phases revealed by the characteristic surface potential do not mean that the preferred specific charge levels would lead to specific Li-vacancy ordering, it is still possible that similar Li vacancy ordering does exist, except that it is smeared at room temperature as a result of thermal fluctuation. In fact, the first-principles calculation predicted that most stable phases of Li vacancy orderings occur only below x=1/2.[10] In this report, we have confirmed that no Li vacancy ordering exists for x ∼ 0.72 at room temperature, based on synchrotron X-

ray Laue diffraction.

While studies on the structure and electrochemical properties of Li_xCoO_2 using polycrystalline sample for the purpose of battery application, physical property exploration using single crystal samples is rare due to its scarce availability. Most of the electronic phase diagrams mapped so far were based on powder samples.[9,11–13] On the other hand, the very few reports based on single crystal samples used either chemical de-intercalation or electrochemical galvanostatic de-intercalation methods,[14] which we will argue in the following as having potential multi-phase issue, not to mention the conclusions drawn from single crystal Li_xCoO_2 samples prepared through ion-exchange route by P2-Na_xCoO_2.[15] In fact, it is highly likely that the inclusion of O2-Li_xCoO_2, instead of the expected O3-Li_xCoO_2, may have occurred through ion-exchanged P2-Na_xCoO_2 original.[16]

Detailed studies based on single crystal sample through the electrochemical potentiostatic de-intercalation route have not been reported so far. The particle size difference and packing density could affect the charging efficiency and surface potential readings for the study based on polycrystalline samples. The common practice of galvanostatic charging based on C-rate in the battery study, i.e., charging rate set on a fraction of the capacity, becomes impractical when there are particularly stable phases existing, instead of a complete solid solution for the ion intercalation. In order to study the electronic phase diagram of Li_xCoO_2 accurately, we report phase studies based on single crystal samples that have been prepared electrochemically using the potentiostatic route, similar to the techniques that have been applied successfully to the P2-Na_xCoO_2 study previously.[17] The potential drawback of surface-versus-bulk difference on the transient galvanostatic scan is avoided, in particular, since sensitive magnetic property interpretation can only be addressed when homogeneous Li (Vacancy) contribution for specific single phase is perfectly isolated without ambiguity. These findings are able to clarify the inconsistency among results obtained through different grain sizes and de-intercalation methods so far.

II. EXPERIMENTAL DETAILS

A complete series of single crystal Li_xCoO_2 sample with x $\sim$ 0.33-0.87 were prepared from electrochemical de-intercalation of the pristine single crystal $Li_{0.87}CoO_2$. The pristine single crystal $Li_{0.87}CoO_2$ was grown using flux method starting from a mixture of $LiCoO_2$: Li_2O_2: LiCl = 1 : 4 : 4, where $LiCoO_2$ was prepared from Li_2CO_3 and Co_3O_4 powder with a molar ratio of Li:Co=1:1 and heated at 900 °C for 24 hours. The mixture was sealed in an alumina crucible using alumina cement, heated to 900 °C, soaked for 5 hours, slowly cooled to 600 °C at a rate of 2 °C/hr, and finally furnace cooled to room temperature. The as-grown single crystal has a

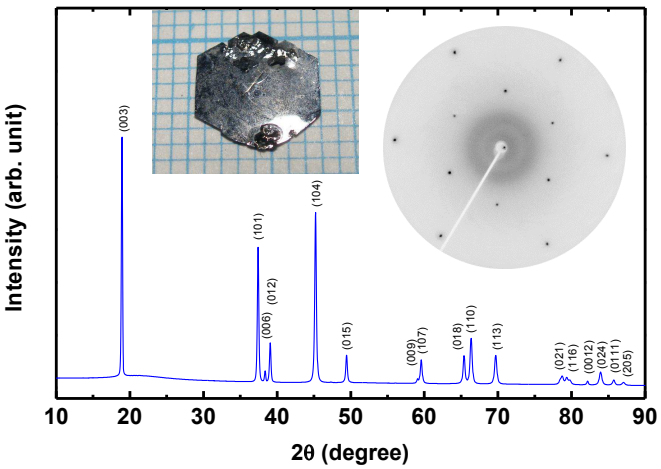

FIG. 2. (color online) Synchrotron X-ray powder diffraction pattern for the as-grown single crystal sample $Li_{0.87}CoO_2$ which has been ground in powder form. All diffraction peaks can be indexed correctly using space group R$\bar{3}$m without extra impurity phases identified. The inset shows the crystal photo and its Laue diffraction pattern of the as-grown single crystal sample.

typical size of $\sim 5\times5\times0.1 mm^3$, with Li content of x $\sim$ 0.87 based on inductively coupled plasma-mass spectrometer (ICP) analysis, which is lower than the expected x=1 due to Li vapor loss under the cement sealing condition. Li content was reduced further through an electrochemical potentiostatic de-intercalation process using various constant applied voltages, where $Li_{0.87}CoO_2$ single crystal was used as working electrode, 1M $LiClO_4$ in propylene carbonate as electrolyte, and Platinum as counter and reference electrodes. All Li contents of Li_xCoO_2 were examined by ICP method to be within error of $\pm$0.01 and verified using the c-axis vs. x plot.[2] Lattice parameters were analyzed using Bruker D-8 diffractometer and the magnetic properties were measured using Quantum Design SQUID-VSM. The single crystal samples of $Li_{0.87}CoO_2$ and $Li_{0.5}CoO_2$ were further examined using Laue diffraction method with synchrotron X-ray generated from 20 keV at the Taiwan-NSRRC.

For the purpose of a detailed electronic phase diagram study on Li_xCoO_2, lithium content and homogeneity has been crucial on its reliability. Besides the lithium content determined and confirmed through ICP analysis plus lattice parameter comparison as described above, the homogeneity of lithium distribution has been examined carefully using synchrotron X-ray diffraction and spin susceptibility analysis. The phase purity and crystal structure of the as-grown single crystal sample has been characterized fully using synchrotron X-ray Laue and powder diffraction as shown in Fig. 2. The as-grown crystal shows hexagonal morphology which is expected for sample possesses hexagonal CoO_2 symmetry within the basal plane. Synchrotron Laue diffraction shown in the inset of

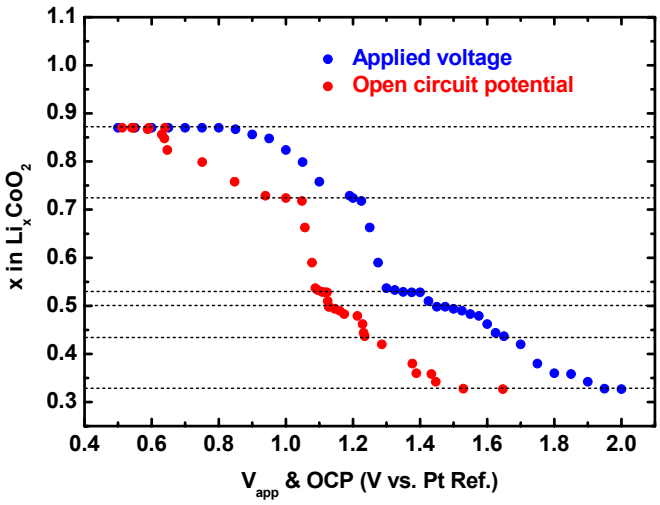

FIG. 3. (color online) Li content x versus applied voltage (V_{app}) and open circuit potential (OCP) for Li_xCoO_2 single crystal electrode. The Li de-intercalation is controlled using potentiostatic process, i.e., a constant V_{app} (vs. Pt reference) is applied to the sample electrode until the induced current falls to the background level, and OCP is recorded after the charging process has ended for 24 hours.

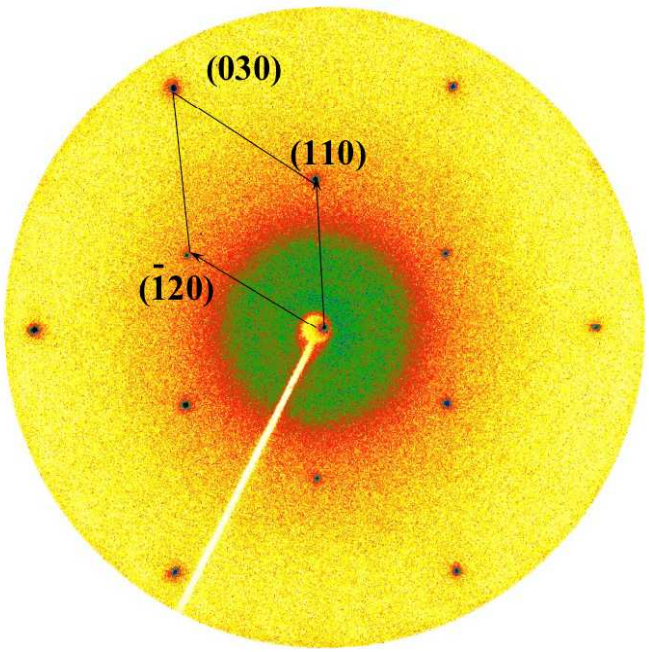

FIG. 4. (color online) Laue diffraction pattern for $Li_{0.72}CoO_2$ obtained using synchrotron X-ray source of wavelength=0.6199Å perpendicular to the CoO_2 layer at room temperature.

Fig.2 confirmed the R$\bar{3}$m symmetry for the crystal perpendicular to the CoO_2 plane with correct index without impurity or superlattice spots. Lithium homogeneity for each x content has been guaranteed through potentiostatic electrochemical de-intercalation method, where the final induced charge transfer current has been saturated for more than 12 hours at the background level to warrant complete conversion for the whole crystal specimen at the designated OCP. X-ray diffraction peak width (FWHM) which reflects lithium homogeneity has been confirmed to be maintained within 0.05±0.01 degree for the whole range of crystal samples studied (not shown).

III. RESULTS AND DISCUSSIONS

A. Electronic phase diagram

In general, open circuit potential (OCP) represents the chemical potential (relative to the reference electrode potential) of a material when the sample acts as a working electrode in the electrochemical cell. The applied overpotential above (or below) the current OCP would induce charge transfer between the electrolyte and the working electrode surfaces, and the induced current decays until OCP is tuned to the new level. The phase diagram mapped by x vs. V as shown in Fig. 3 reveals several stable phases from the plateau of x vs. V, which closely correlate with the specific Li contents near ∼ 0.72, 0.53, 0.50, 0.43, and 0.33. Although the stacking sequences between alkali metal and CoO_2 layers and the space group are different between Na_xCoO_2 and Li_xCoO_2, the basic character of the x vs. V plot for Li_xCoO_2 is very similar to that found for Na_xCoO_2.[2,9,13] It is not surprising to find phases with x ∼ 1/2 and 1/3 when both systems have similar CoO_2 networks of 2D triangular lattice. In addition, in proximity to the exact half filling, there are metastable phases of x ∼ 0.53 and 0.43 found for Li_xCoO_2. Similar phases have also been identified in Na_xCoO_2 near x ∼ 0.55 and 0.43 as reported earlier.[17,18]

Although P2-Na_xCoO_2 and O3-Li_xCoO_2 have different gliding sequences and alkaline metal ion environments as shown in Fig. 1, it is interesting to find that $Li_{0.72}CoO_2$ shows particular stability similar to the fully characterized stable phase of $Na_{0.71}CoO_2$. $Na_{0.71}CoO_2$ has been identified by synchrotron Laue X-ray with a proposed simple hexagonal $\sqrt{12}$a×$\sqrt{12}$a×3c superstructure model formed by Na vacancy multivacancy clusters before.[6,19,20] Na vacancy level that leads to the x=0.71 phase formation is a result of perfect tri- and quadri-vacancy stacking in the space group of $P6_3/mmc$ symmetry (or $P3_1$ after Na ordering is considered), i.e., closely related to the necessity of inversion symmetry between the nearest-layer oxygen positions. While Li_xCoO_2 has been described in the space group of R$\bar{3}$m with CoO_2 layers to glide along the [111] direction of three Li-CoO_2 per unit in the hexagonal description as shown in Fig. 1, the Li vacancy level that is responsible for the existence of x ∼ 0.72 stable phase is puzzling.

To search for the possible Li vacancy ordering, Laue

pattern for $Li_{0.72}CoO_2$ obtained using synchrotron X-ray is shown in Fig. 4. While the transmission Laue is taken perpendicular to the CoO_2 layer, a clear hexagonal symmetry can be indexed. Comparing with the Laue pattern of $Na_{0.71}CoO_2$ with well-defined $\sqrt{12}$a hexagonal superlattice,[6] no superlattice can be identified besides the main low indexing (hk0) planes constructed by the hexagonal Co network of a=2.8156 $\AA$. Contrary to the $Na_{0.71}CoO_2$ superlattice, which is required by the Na trimer formation under $P6_3/mmc$ symmetry, $Li_{0.72}CoO_2$ has no similar symmetry condition, but, on the other hand, sits close to the phase boundary of the two-phase region between ∼0.75-0.94 as reported previously.[2,9,21] The phase of relatively shorter c-axis of the two-phase could be related to the partial O2-like gliding as suggested by Carlier *et al.* for the P2- to O2- structural transition.[16] It is possible that the particular stability of $Li_{0.72}CoO_2$ may have nothing to do with specific Li vacancy ordering, but rather closely related to the requirement of missing O2-like gliding after the screening effect is weakened by the lower Li level between the CoO_2 blocks.

It is very difficult to obtain single phase $Li_{0.72}CoO_2$ using potentiostatic method without going through an extreme fine tuning process on applied voltage, mostly because it sits between the 0.75-0.94 two-phase region (to be discussed in the following sections), and the steep and narrow voltage range for 0.72-0.52 phase formation as shown in Fig. 3. Li-Co chemical disordering has also been ruled out based on the finite-temperature calculation results,[22] although supporting evidence has been found experimentally in the literature.[23] The average diffusion coefficient at room temperature obtained from polycrystalline Li_xCoO_2 is in the order of D_{Li}∼ 10^{-12},[24] which is nearly four orders lower (D_{Na}∼10^{-8} cm^2/s) than that of Na_xCoO_2 estimated from single crystal study,[18] except that the minima of D_{Na}'s near those specifically stable phases of x ∼ 0.71, 0.50, and 0.33 fall to the same average level as D_{Li}. Although the reported D_{Li} values in the literature vary from 10^{-13}-10^{-7} and the differences have been attributed to the assumption of geometrical factors used in the calculation,[24] it is still possible that the specific Li vacancy level of Li_xCoO_2 does not induce enough chemical potential reduction for potential ionic ordering mechanism, as demonstrated by the missing of Li vacancy ordering for $Li_{0.72}CoO_2$.

Based on OCP studies for Li_xCoO_2 sample electrode as shown in Fig.3, there are two extra phases in proximity to the exact half filling of x = 0.5, i.e., the two distinguishable stable phases revealed by the narrow plateau near ∼ 0.53 and 0.43, which have also been observed under galvanostatic scan previously.[24,25] These two specific x values are close to those found in Na_xCoO_2 system near x ∼ 0.55 and 0.43 with distinctly different Laue superlattice patterns and magnetic phase transitions.[17] The origin of phases with slight deviation from exact x=1/2 remains to be explored, but preliminary electron diffraction studies for Na_xCoO_2 with x near 0.5 has been attributed to the metastable phases in proximity to the exact half-filling as a result of alternating vacancy rich/poor 1D Na zigzag chains.[26]

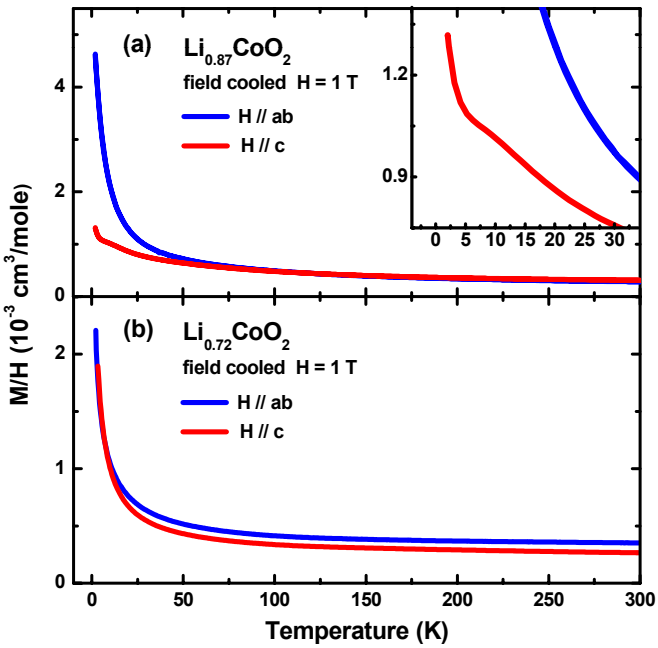

FIG. 5. (color online) Magnetic susceptibilities for $Li_{0.87}CoO_2$ and $Li_{0.72}CoO_2$ single crystals. The inset reveals the anisotropic anomaly near ∼10K, which suggests the existence of A-type AF ordering with spins aligned antiferromagnetic along the c-direction.

B. Magnetic susceptibilities

Magnetic susceptibilities for Li_xCoO_2 (x ∼ 0.87, 0.72) single crystals are summarized in Fig. 5. These results differ significantly from those reported previously based on either powder or single crystal samples prepared with chemical or galvanostatic de-intercalated methods.[13,15] We find that the signal size of magnetic anomalies revealed by the sensitive SQUID magnetometry on single crystal samples are very weak, which cannot be reliably observed in polycrystalline samples, especially when inhomogeneity cannot be ruled out in chemical or galvanostatic de-intercalation processes. Besides, magnetic impurity of Co_3O_4 may become dominant below 50K under certain annealing conditions and the muon spin resonance tool shows limited sensitivity in this range.[27,28]

As shown in Fig. 5(a), the anisotropic magnetic anomaly found near ∼10K for the as-grown $Li_{0.87}CoO_2$ clearly indicates the existence of possible A-type antiferromagnetic ordering, similar to that found previously in Na_xCoO_2 for x ∼ 0.82-86, where the magnetization is reduced for H‖c to signal antiparallel spin arrangement in c-direction.[7,17] The A-type antiferromagnetic (A-AF) or-

dering for $Na_{0.82}CoO_2$ has been confirmed through neutron scattering experiment before,[29] where the interlayer AF coupling coexists with an in-plane ferromagnetism (FM) of itinerant electron spins.[6] The similar finding of A-AF behavior in the as-grown $Li_{0.87}CoO_2$ is not surprising, although it has not been observed through magnetic susceptibility measurement before to the best of our knowledge.

The magnetic susceptibilities for $Li_{0.72}CoO_2$ shown in Fig. 5(b) demonstrate similar magnetic behavior to that of $Na_{0.71}CoO_2$ also, i.e., no magnetic anomaly has been found between 1.7-300K, which is in great contrast to the finding of 175K phase transition reported previously.[9,15,28] Hertz *et al.* have examined the confusing 175K anomaly carefully before and ruled out the possibility of the existence of Co-O impurities. In addition, the observed aging effect of 175K anomaly strongly implies the occurrence of magnetic moment induced by local microscopic Li inhomogeneity.[9] We suspect that Li inhomogeneity becomes the major problem for samples prepared using chemical or galvanostatic de-intercalation methods. This can also be argued from the persistent observation of the 175K phase transition with various intensities found in the whole range of x $\sim$ 0.78-0.46, a typical example of possible inclusion of identical impurity phase with strong magnetic signal contribution.[9,15] On the other hand, our single crystal samples were prepared with well-controlled potentiostatic de-intercalation method to warrant Li homogeneity until there was no difference on the potential reading between surface and the bulk. Besides, there are two different c-axes detected in the range of $\sim$0.72-1 before single phase formation below $\sim$ 0.72 as reported by various preparation methods and summarized in Fig. 6. A first order metal-insulator Mott transition has also been proposed for x $\lesssim$ 0.75 based on density function theory (DFT) calculations, which could be closely related to the two phase coexistence in the same range as a result of gradual de-localization from x $\gtrsim$ 0.95.[30] Phase purity requirement for the physical property investigation becomes crucial when Li inhomogeneity cannot be controlled easily, especially when electrochemical process can only detect the surface potential.

Curie-Weiss law fitting for the paramagnetic behavior of the spin susceptibilities for $Li_{0.72}CoO_2$ shows that Curie constant is $\sim$ 0.011 cm^3-K/mole, which is nearly one tenth of that for $Na_{0.71}CoO_2$ reported previously.[6] The significantly lower level of localized spins suggests that the doped holes resulting from Li vacancy are mostly mobile. This observation is consistent with the absence of Li vacancy ordering in the synchrotron Laue photograph, while superlattice ordering of Na vacancy cluster has been proposed to create more localized spins near the vacancy cluster centers and the rest of the doped holes are itinerant.[6,31] The absence of magnetic ordering for the local moment on a frustrated lattice has been suggested to be a unique spin liquid state for $Na_{0.71}CoO_2$. Similar behavior for $Li_{0.72}CoO_2$ deserves further investigation also.

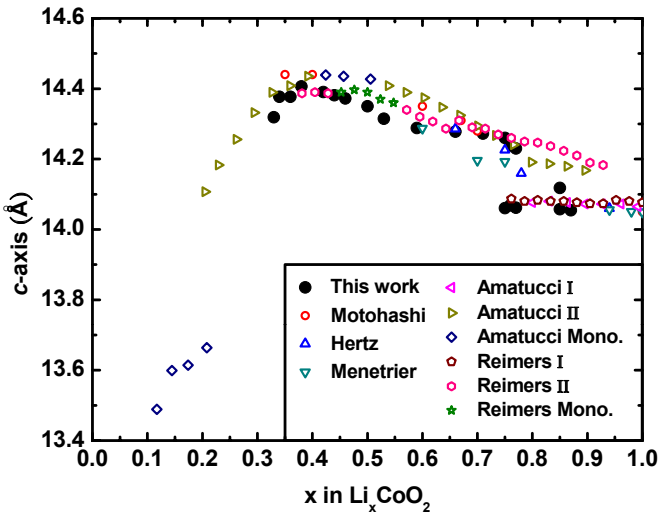

FIG. 6. (color online) c-axes for single crystal samples studied in this work (solid circle) are compared with those reported in the literature (empty symbols).[2,9,13,21,32] Monoclinic structure distortion has been observed for Li_xCoO_2 close to x $\sim$ 0.5 and 0.2.

C. Crystal structures

The c-axis lattice parameters from five published works plus our current results are summarized in Fig. 6.[2,9,13,21,32] We note that the as-grown single crystal $Li_{0.87}CoO_2$ falls in the reported two-phase region; however, the as-grown crystal is clearly single phase with smaller c-axis, similar to those for x $\gtrsim$0.95. The two-phase phenomenon must be coming from the domain-like de-intercalation process before x$\lesssim$0.72 is achieved, which should occur only in the de-intercalation process at room temperature but not through the melt growth condition at high temperatures, as additionally verified by the two-phase observation in our crystal samples of 0.72$\lesssim$x$\lesssim$0.87 obtained by following electrochemical de-intercalation. The main reason for the persistent two-phase for x$\sim$0.72-1 has been proposed theoretically to be a first order metal-insulator transition as a Mott transition of impurities, where high mobility of Li vacancies allows the $\sim$25% vacancy metallic phase to grow at the expense of insulating phase of x$\gtrsim$0.95 at room temperature.[30] It is noted that c-axes values for 0.33$\lesssim$ x $\lesssim$0.72 obtained in this study (Fig. 6) are consistently lower than those widely distributed values reported previously.[2,21] Li inhomogeneity in powder samples is a reasonable assumption to explain the difference, i.e., it is highly likely that the Li contents were over-estimated before as a result of surface-to-bulk potential difference during de-intercalation process for the powder sample, i.e., possibly with mixture of low x phases which are closer to x$\lesssim$0.5 at the grain boundaries, especially when galvanostatic de-intercalation route has been applied.

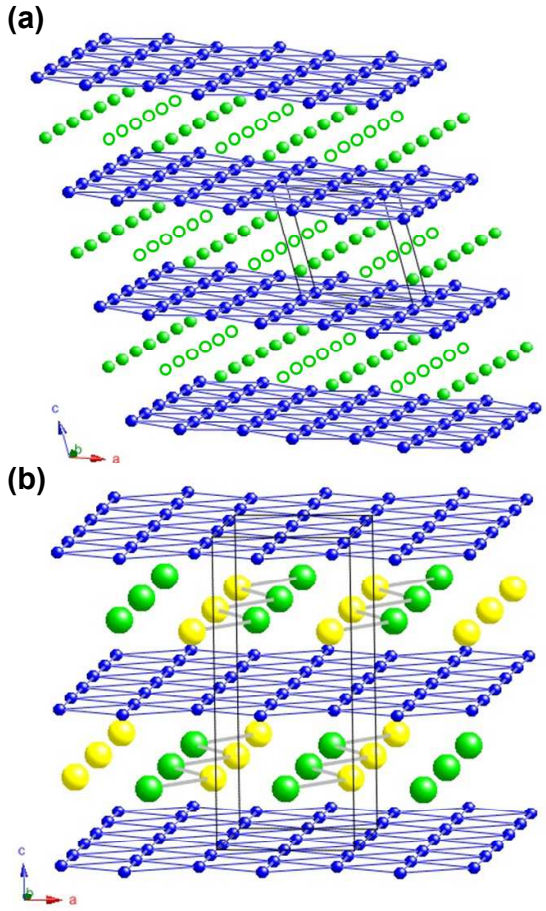

FIG. 7. (color online) Crystal structures of (a) $Li_{0.5}CoO_2$ described in P2/m,[33] where solid and empty circles in green represent Li and Li-vacancy respectively, and (b) $Na_{0.5}CoO_2$ with Na sublattice described in space group of Pnmm[35], where zigzag chains formed by Na1 (green) and Na2 (yellow) solids have been defined in the original $P6_3/mmc$ symmetry.

D. Monoclinic $Li_{0.5}CoO_2$

Monoclinic distortion has been observed previously in Li_xCoO_2 close to x∼0.5 and 0.2 at room temperatures.[2,21] The crystal structure of $Li_{0.5}CoO_2$ has been identified as monoclinic lattice with space group $P2/m$.[33,34] The gliding blocks of CoO_2 and Li for Li_xCoO_2 with $R\bar{3}m$ symmetry of three Li-CoO_2 layers per unit must favor the monoclinic distortion when Li content is reduced to half. In addition, the alternating linear Li-vacancy chains for $Li_{0.5}CoO_2$ is quite different from the zigzag Na chain in $Na_{0.5}CoO_2$.[35] Li in O3-Li_xCoO_2 has only one site, which sits directly beneath the Co column, similar to the Na1 site in P2-Na_xCoO_2.[6] But when cation vacancy is generated through de-intercalation, Na ion can move from the originally energetically favorable Na2 site to the now energetically more favorable Na1 site to form Na-trimer or multi-vacancy cluster,[5] which is not a possible mechanism under Li_xCoO_2 $R\bar{3}m$ symmetry, and an alternative Monoclinic distortion mechanism is chosen. In fact, mazed domain structure of monoclinic $Li_{0.5}CoO_2$ has been revealed through electron diffraction before, where equivalent domains of in-plane Li-vacancy ordering and other nm size domains of variants exist.[33]

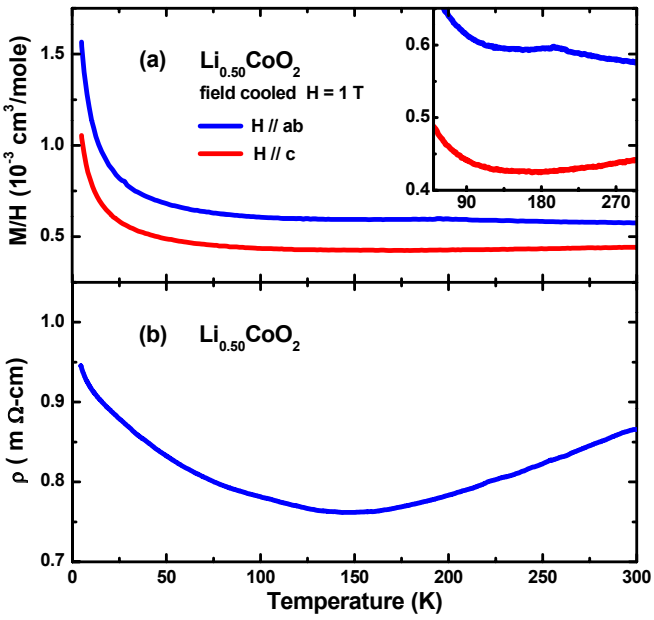

FIG. 8. (color online) (a) Magnetic susceptibility for $Li_{0.5}CoO_2$ single crystal measured using 1 Tesla for H‖ab and H‖c, and the transition region near ∼200K enlarged in the inset. (b) The in-plane resistivity for x=0.5.

The magnetic susceptibility and resistivity measurement results for $Li_{0.5}CoO_2$ are shown in Fig. 8. There is a small dip of susceptibility found near ∼ 200K for H‖ab only as revealed in the inset of Fig. 8(a), but no corresponding anomaly found for H‖c, which is similar to the behavior of antiferromagnetic transition near ∼ 88K found in $Na_{0.5}CoO_2$. This AF spin ordering for $Na_{0.5}CoO_2$ has been proposed to be coming from the alternating rows of AF ordered and nonordered Co ions within the ab-plane.[36] Columns of alternating Li-vacancy for $Li_{0.5}CoO_2$ is shown in Fig. 7(a).[33,34] The anisotropic anomaly near ∼ 200K for $Li_{0.5}CoO_2$ could be coming from a similar AF ordering, and spin polarized neutron scattering should be performed to check this possibility. For $Na_{0.5}CoO_2$ shown in Fig. 7(b), the intricate Co columns sandwiched between upper and lower zigzag Na chains must form the ordered Co with AF spins, while the in-between Co columns are spinless as supported by the neutron scattering study results.[36] Similarly, $Li_{0.5}CoO_2$ also possesses alternating Li-vacancy columns and the nearby Co columns must generate similar ordered AF ordered spins and non-ordered spinless columns in the hexagonal Co-plane.

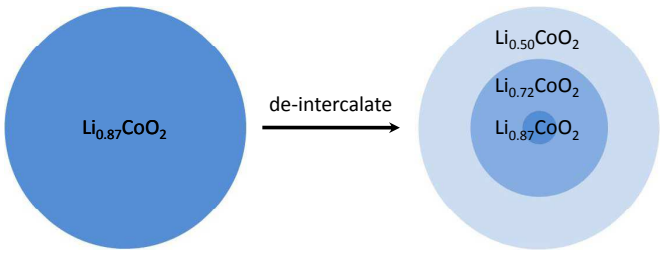

FIG. 9. (color online) Radial model of inhomogeneous galvanostatic or chemical de-intercalation for Li_xCoO_2.

Although there is a significant metal-to-insulator transition follows at ∼51K for $Na_{0.5}CoO_2$, there is only a very weak increase of resistivity found below ∼150K for $Li_{0.5}CoO_2$. The metal-insulator transition below ∼ 51K for $Na_{0.5}CoO_2$ has been attributed to the charge localization as a result of delicate balance between local Coulomb repulsion and kinetic energy in the CoO_2 plane when ideal interpenetrating filled (spinless) and half-filled (with spin) orthorhombic sub-lattices are constructed.[37] On the other hand, there is no clear metal-to-insulator transition observed down to 4.2K for $Li_{0.5}CoO_2$, except a resistivity minimum occurs near ∼150K as shown in Fig. 8(b). Unlike the maintained Na zigzag chain ordering along the c-direction for $Na_{0.5}CoO_2$, the monoclinic distortion for $Li_{0.5}CoO_2$ along c-axis must be responsible for the missing charge ordering when 3D ordering along c-direction is broken.

E. De-intercalation and Li homogeneity

It has been puzzling to find that there is one persistent phase that can be identified through several experimental techniques near ∼150-175K within a wide range of x ∼ 046-0.78 as summarized in Table I. In addition, the observed 175K phase anomaly shows a significant thermal hysteresis in both resistivity and magnetic susceptibility measurements.[13,15] The persistent existence of one phase signature in a wide range of lithium content suggests that such phase has not been isolated completely from the co-existing phase mixture. The observation of thermal hysteresis also strongly suggests that such hard-to-extract phase could be closely related to a phase existence within extremely narrow phase space, i.e., slight deviation due to inhomogeneity could create phase separation of small miscibility gap. In fact, Hertz *et al.* have proposed that the detected 175K anomaly could be associated with a phase that can only be stabilized at the surface or grain boundaries, as suggested by its aging character and mostly found in powder samples.[9] Examine the electronic phase diagram mapped by the potentiostatic de-intercalation method as shown in Fig. 3, we find that indeed there exists a sharp x vs V slope within ∼20 mV for sample preparation of x∼0.52-0.72, i.e., small deviation on applied potential would produce two-phase coexistence unless post annealing at 120°C is applied. We failed to isolate the expected phase that shows similar 175K anomaly after repeated careful tuning of V_{app} near ∼125 mV following the electronic phase diagram shown in Fig. 3,. Although these negative results cannot exclude the existence of a phase that shows ∼175K anomaly as revealed by several experimental techniques, which strongly supports that this peculiar phase must exist within a extremely narrow phase space to be isolated cleanly or associate with surface and grain boundaries closely.

Most early studies of Li_xCoO_2 phase diagram used galvanostatic scans on polycrystalline samples in electrochemical battery cells, and the stable phases were isolated using the characteristic surface potential and X-ray diffraction. The battery construction using fine polycrystalline sample is efficient for revealing the occurrence of stable phases through surface potential with total charge estimated using Faraday's law. Alternatively, chemical de-intercalation using oxidant under various concentrations can also serve the same purpose, as summarized in Table I. However, these processes are of approximation for a quasi-equilibrium process at the limited time scale, i.e., unless the charging rate of galvanostatic current density is lower than the Li diffusion rate, and the charging process can be stopped immediately after reaching the targeted levels. Strictly speaking, galvanostatic de-intercalation method cannot guarantee single phase formation with accurate charge integration, especially when multiple stable phases continue to build up on the outer layers of the particle, yet only the surface potential is recorded. Radial and Mosaic models have been proposed to describe the intercalation problem for the battery electrode material Li_xFePO_4 with only two stable phases of x = 1 and 0,[42] but there are more stable phases identified in Li_xCoO_2 as proposed in Fig. 9 following a Radial model description. It is demonstrated that the delithiation process cannot be a complete process in the galvanostatic scan, i.e., there is always remanent stable phases in the inner core area that cannot be reached in time galvanostatically when the charging current is terminated by the achieved surface potential before diffusion process is completed.

IV. CONCLUSIONS

In summary, by using a series of potentiostatically de-intercalated single crystal Li_xCoO_2, we find great similarity between electronic phase diagrams of Na_xCoO_2 and Li_xCoO_2. Contrary to most reports based on powder sample prepared with galvanostatic or chemical de-intercalation methods, current work revealed an A-type antiferromagnetic signature for x ∼ 0.87 and the non-existence of magnetic ordering down to 1.7K for x ∼ 0.72. Although $Li_{0.72}CoO_2$ shows similar stoichiometry and particular stability compared to $Na_{0.71}CoO_2$ with well-

TABLE I. Summary of Li_xCoO_2 samples prepared with different de-intercalation routes

Reference	deintercalation method	powder/crystal	175K anomaly
Imanishi *et al.* 1999[38]	chemical	powder	x∼0.76-0.61
Menetrier *et al.* 1999[32]	EC galvanostatic	powder	N.A.
Clemencon *et al.* 2007[25]	EC galvanostatic	powder	N.A.
Mukai *et al.* 2007[11]	EC galvanostatic	powder	x∼0.75-0.50
Hertz *et al.* 2008[9]	chemical	powder	x∼0.78-0.51
Kawasaki *et al.* 2009[39]	EC galvanostatic	powder	N.A.
Sugiyama *et al.* 2009[28]	EC galvanostatic	powder	x∼0.73-0.53
Motohashi *et al.* 2009[13]	EC galvanostatic	powder	x∼0.70-0.50
Mohanty *et al.* 2009[40]	chemical	powder	no
Miyoshi *et al.* 2010[15]	ion exchange+chemical	single crystal	x∼0.71-0.46
Ishida *et al.* 2010[41]	ion exchange+chemical	thin film	x∼0.66
This work	EC potentiostatic	single crystal	no

defined Na vacancy superlattice ordering, the former does not possess any Li vacancy ordering. Near half filling of Li, three phases of x $\sim$ 0.53, 0.50, and 0.43 have been identified and isolated to show distinct physical properties. Comparing with $Na_{0.5}CoO_2$, no metal-insulator transition has been found for $Li_{0.5}CoO_2$, although similar antiferromagnetic ordering is implied below $\sim$ 200K. Based on a Radial model interpretation, current potentiostatic study results based on single crystal samples support that the widely observed within x $\sim$ 0.75-0.50 but hard-to-extract phase with a magnetic anomaly near $\sim$ 175K could be related to a minor phase sitting preferentially on the surface or grain boundaries.

ACKNOWLEDGMENT

FCC acknowledges the support from National Science Council of Taiwan under project number NSC-99-2119-M-002-011-MY2.

* fcchou@ntu.edu.tw

[1] J. B. Goodenough and Y. Kim, Chem. Mater. **22**, 587 (2010).
[2] G. G. Amatucci, J. M. Tarascon, and L. C. Klein, J. Electrochem. Soc. **143**, 1114 (1996).
[3] K. Takada, H. Sakurai, E. T. Muromachi, F. Izumi, R. A. Dilanian, and T. Sasaki, Nature **422**, 53 (2003).
[4] M. L. Foo, Y. Wang, S. Watauchi, H. W. Zandbergen, T. He, R. J. Cava, and N. P. Ong, Phys. Rev. Lett. **92**, 247001 (2004).
[5] M. Roger, D. J. P. Morris, D. A. Tennant, M. J. Gutmann, J. P. Goff, J.-U. Hoffmann, R. Feyerherm, E. Dudzik, D. Prabhakaran, A. T. Boothroyd, N. Shannon, B. Lake, and P. P. Deen, Nature **445**, 631 (2007).
[6] F. C. Chou, M.-W. Chu, G. J. Shu, F.-T. Huang, W. W. Pai, H. S. Sheu, and Patrick A. Lee, Phys. Rev. Lett. **101**, 127404 (2008).
[7] G. J. Shu, F.-T. Huang, M.-W. Chu, J.-Y. Lin, Patrick A. Lee, and F. C. Chou, Phys. Rev. B **80**, 014117 (2009).
[8] G. J. Shu, W. L. Lee, F.-T. Huang, M.-W. Chu, Patrick A. Lee, and F. C. Chou, Phys. Rev. B **82**, 054106 (2010).
[9] J. T. Hertz, Q. Huang, T. McQueen, T. Klimczuk, J. W. G. Bos, L. Viciu, and R. J. Cava, Phys. Rev. B **77**, 075119 (2008).
[10] A. Van der Ven, M. K. Aydinol, G. Ceder, G. Kresse, and J. Hafner, Phys. Rev. B **58**, 2975 (1998).
[11] K. Mukai, Y. Ikedo, H. Nozaki, J. Sugiyama, K. Nishiyama, D. Andreica, A. Amato, P. L. Russo, E. J. Ansaldo, J. H. Brewer, K. H. Chow, K. Ariyoshi, and T. Ohzuku, Phy. Rev. Lett **99**, 087601 (2007).
[12] J. Sugiyama, H. Nozaki, J. H. Brewer, E. J. Ansaldo, G. D. Morris, and C. Delmas, Phy. Rev. B **72**, 144424 (2005).
[13] T. Motohashi, T. Ono, Y. Sugimoto, Y. Masubuchi, S. Kikkawa, R. Kanno, M. Karppinen, and H. Yamauchi, Phys. Rev. B **80**, 165114 (2009).
[14] K. Miyoshi, C. Iwai, H. Kondo, M. Miura, S. Nishigori, and J. Takeuchi, J. Phys.: Conf. Ser. **150**, 042129 (2009).
[15] K. Miyoshi, C. Iwai, H. Kondo, M. Miura, S. Nishigori, and J. Takeuchi, Phys. Rev. B **82**, 075113 (2010).
[16] D. Carlier, I. Saadoune, L. Croguennec, M. Menetrier, E. Suard, and C. Delmas, Solid State Ionics **144**, 263(2001).
[17] G. J. Shu, A. Prodi, S. Y. Chu, Y. S. Lee, H. S. Sheu, and F. C. Chou, Phys. Rev. B **76**, 184115 (2007).
[18] G. J. Shu and F. C. Chou, Phys. Rev. B **78**, 052101 (2008).
[19] F.-T. Huang, M.-W. Chu, G. J. Shu, H. S. Sheu, C. H. Chen, L.-K. Liu, Patrick A. Lee, and F. C. Chou, Phys. Rev. B **79**, 014413 (2009).
[20] F.-T. Huang, A. Gloter, M.-W. Chu, F. C. Chou, G. J. Shu, L.-K. Liu, C. H. Chen, and C. Colliex, Phys. Rev. Lett. **105**, 125502 (2010).
[21] J. N. Reimers and J. R. Dahn, J. Electrochem. Soc. **139**, 2091 (1992).
[22] C. Wolverton and A. Zunger, Phys. Rev. Lett. **81**, 606 (1998).
[23] M. Menetrier, D. Carlier, M. Blangero, and C. Delmas, Electrochemical and Solid-State Letters, **11**, A179 (2008).

[24] Y.-I. Jang, B. J. Neudecker, and N. J. Dudney, Electrochemical and Solid-State Letters, **4**, A74 (2001).
[25] A. Clemencon, A.T. Appapillai, S. Kumar, and Y. Shao-Horn, Electrochimica Acta **52**, 4572 (2007).
[26] F.-T. Huang *et al.*, unpublished.
[27] A. Artemenko, M. Menetrier, M. Pollet, and C. Delmas, J. Appl. Phys. **106**, 064914 (2009).
[28] J. Sugiyama, K. Mukai, Y. Ikedo, H. Nozaki, M. Mansson, and I. Watanabe, Phys. Rev. Lett. **103**, 147601 (2009).
[29] S. P. Bayrakci, C. Bernhard, D. P. Chen, B. Keimer, R. K. Kremer, P. Lemmens, C. T. Lin, C. Niedermayer, and J. Strempfer, Phys. Rev. B **69**, 100410(R) (2004).
[30] C. A. Marianetti, G. Kotliar, and G. Ceder, Nature materials **3**, 627 (2004).
[31] L. Balicas, Y. J. Jo, G. J. Shu, F. C. Chou, and Patrick A. Lee, Phys. Rev. Lett. **100**, 126405 (2008).
[32] M. Menetrier, I. Saadoune, S. Levasseur, and C. Delmas, J. Mater. Chem. **9**, 1135 (1999).
[33] Y. Shao-Horn, S. Levasseur, F. Weill, and C. Delmas, J. Electrochem. Soc. **150**, A366 (2003).
[34] Y. Takahashi, N. Kijima, K. Dokko, M. Nishizawa, I. Uchida, and J. Akimoto, J. Sol. St. Chem. **180**, 1020 (2007).
[35] Q. Huang, M. L. Foo, R. A. Pascal, Jr., J. W. Lynn, B. H. Toby, Tao He, H. W. Zandbergen, and R. J. Cava, Phys. Rev. B **70**, 184110 (2004).
[36] G. Gasparovic, R. A. Ott, J.-H. Cho, F. C. Chou, Y. Chu, J. W. Lynn, and Y. S. Lee, Phys. Rev. Lett. **96**, 046403 (2006).
[37] T.-P. Choy, D. Galanakis, and P. Phillips, Phys. Rev. B **75**, 073103 (2007).
[38] N. Imanishi, M. Fujiyoshi, Y. Takeda, O. Yamamoto, and M. Tabuchi, Solid State Ionics **118**, 121 (1999).
[39] S. Kawasaki, T. Motohashi, K. Shimada, T. Ono, R. Kanno, M. Karppinen, H. Yamauchi, and G. Q. Zheng, Phys. Rev. B **79**, 220514(R) (2009).
[40] D. Mohanty and H. Gabrisch, ECS Transations **19**, 25 (2009).
[41] Y. Ishida, A. Mizutani, K. Sugiura, H. Ohta, and K. Koumoto, Phys. Rev. B **82**, 075325 (2010).
[42] A. S. Andersson and J. O. Thomas, Journal of Power Sources **97-98**, 498 (2001).